

Improved algorithm for detecting cloud layers and amounts using retrievals from a surface-based multifrequency profiling radiometer

Pierre Bouchard*

Communications Research Centre Canada, 3701 Carling Ave., Ottawa, Ontario, Canada K2H 8S2

ABSTRACT

This paper will explore the possibility of using vertical profiles of temperature and relative humidity retrieved by a surface-based multifrequency profiling radiometer to determine the bases and tops of clouds as well as amounts (sky cover) of individual layers using a technique originally developed by Chernykh and Eskridge (CE) for radiosonde profiles. The CE method determines the presence of cloud layers by monitoring the second derivative of temperature $T(z)$ and relative humidity $R(z)$ vertical profiles. Necessary conditions for detection of cloud layers are: $T''(z) \geq 0$ and $R''(z) \leq 0$. We have improved this algorithm by using supplementary retrieved data not measured by radiosondes: the cloud base height estimated by an infrared thermometer and the liquid water path L . This extra set of conditions can be summarized as follows: a cloud contains liquid water whenever the retrieved L exceeds a certain threshold value and its cloud base height is lower than some maximum value. The cloud amount is estimated using the minimum dewpoint depression within the detected layer and the corresponding temperature. This dependence of cloud amount on dewpoint depression and temperature is presented in the form of a new Arabeby diagram empirically derived for the liquid water and mixed-phase cloud climatology of the Ottawa area. Comparisons will be made between predictions based on this improved cloud detection algorithm for low and midlevel clouds as well as cases of clear skies and co-located "ground truth" surface observations using daytime data collected in Ottawa between the fall of 2004 and the summer of 2005. These sky observations are based on WMO Cloud Atlas descriptions supplemented by hourly surface observations of cloud cover from the Ottawa Airport. Our new algorithm has been shown to significantly reduce the number of false positives.

Keywords: Cloud detection, microwave radiometry, temperature and humidity profiles.

1. INTRODUCTION

A few years ago, the Communications Research Centre Canada (CRC) in Ottawa acquired a multifrequency profiling radiometer (Radiometrics TP/WVP-3000) to study and model the impact of clouds and water vapour on satellite links above about 30 GHz. It uses 12 channels, five in the K-band between 22.235 and 30 GHz for water vapour profiling and seven in the V-band between 51.25 and 58.8 GHz for temperature profiling. Both K-band and V-band receivers are located in the same cabinet and share the same antenna and pointing systems. It also features an infrared thermometer (operating between 9.6 and 11.5 μm) directed downward to a gold plated mirror that reflects energy from the zenith, thereby detecting the cloud base temperature. Thus the height of the cloud base can be obtained using the contemporaneous retrieved temperature profile of the lowest layer.

Since ice has negligible absorption at these twelve frequencies and therefore has negligible emission, Cirrus clouds - usually entirely composed of ice crystals - are not detected by the profiling radiometer.

The profiling radiometer can retrieve vertical profiles of temperature, absolute as well as relative humidity and cloud liquid water every 30 seconds or every minute from the surface up to 10 km in height under clear sky and cloudy conditions. Higher sampling frequencies (e.g., retrieving 21 profiles in five minutes) are also currently available. Its vertical resolution changes with altitude: it is 100 m between the ground and 1 km and 250 m between 1 km and 10 km. It has automated elevation-scanning capability and is also capable of assessing the columnar cloud liquid water content

* Pierre.Bouchard@crc.ca; phone +613 998-2441; fax +613 990-6339; www.crc.ca.

(also known as the liquid water path L) continuously, unlike what can be achieved with radiosondes. This profiling radiometer also measures surface temperature, pressure and relative humidity continuously. Finally the water vapour path (V) is also retrieved at the same sampling frequency as the various profiles.

Using retrieved profiles as input data to detect cloud layers and assess their sky cover clearly offers several advantages over a radiosonde-based method. It provides continuous and unattended measurements of the first 10 km of the troposphere made every minute. True zenith profiles can be used as input data that are free from uncontrolled horizontal drift through the atmosphere.

This paper will explore the possibility of using vertical profiles of temperature and relative humidity retrieved by this microwave radiometer to determine the bases and tops of clouds as well as amounts of individual layers (percentage of sky cover) using a technique originally developed by I.V. Chernykh and R.E. Eskridge¹ for radiosonde profiles. Hereafter the method will be referred to as the Chernykh and Eskridge (CE) method.

The CE method detects the presence of cloud layers by monitoring the second order derivative of temperature $T(z)$ and relative humidity $R(z)$ vertical profiles. Conditions for detection of cloud layers are: $T''(z) \geq 0$ and $R''(z) \leq 0$. The cloud amount in percent is then estimated using the minimum dewpoint depression (i.e., the difference between the temperature at a given level and the corresponding dew point temperature) within the detected cloud layer and the corresponding temperature at that level. The dependence of cloud amount on dewpoint depression and temperature is presented in the form of the so-called Arabey diagram² based on radiosonde data from the mid-latitudes of Eurasia and the tropical latitudes of the Indian Ocean.

Comparisons will be made for low and middle cloud layers between predictions based on the CE method using radiometric profiles and “ground truth” surface observations consisting of our own co-located sky observations at CRC (based on the WMO International Cloud Atlas descriptions) supplemented by hourly cloud data from the Ottawa International Airport (a facility equipped with a ceilometer). These comparisons will include cases of low and middle cloud layers as well as cases of clear skies. Improvements to the CE method will also be described, most notably a new empirically-derived Arabey diagram for the water and mixed-phase cloud climatology of the Ottawa area as well as the use of retrieved data not measured by radiosondes to reduce the number of false positives: the cloud base height estimated by a zenith-pointing infrared thermometer and the liquid water path L .

2. METHODOLOGY

2.1 Introduction

Cloud layers affect temperature (T) and relative humidity (R) in the atmosphere. Therefore any instrument measuring temperature and humidity profiles – either a radiosonde or a profiling radiometer – will record variations in the readings of these parameters at the altitudes where clouds exist in the atmosphere. In the case of radiosondes, the response of thermistors and hygristors to cloudy layers may sometimes have little effect on the absolute values of the measured quantities due to inertia, but these layers nearly always manifest their presence in relative changes, i.e. derivatives of T and R with respect to height.

Although physically sound, the CE method was originally developed from a purely statistical analysis of radiosonde profiles. Chernykh and Eskridge noticed that characteristic features in temperature and humidity profiles inside and outside cloudy layers were more distinct (i.e. had larger magnitudes) in the second derivatives $T''(z)$ and $R''(z)$ with respect to height z than either the first derivatives ($T'(z)$ and $R'(z)$) or the parameter values themselves³ ($T(z)$ and $R(z)$).

The original CE method is described as follows in Section 2.2^{1,3}.

2.2 Original CE method

Temperature (T) and relative humidity (R) profiles are first approximated by natural cubic splines $S(x)$ ⁴ (with boundary conditions $S''(a) = S''(b) = 0$) in order to have continuous second derivatives over the entire profiles. Their second derivatives $T''(z)$ and $R''(z)$ are therefore piecewise linear functions of altitude z . Interpolation using cubic splines also smoothes out the high-frequency “noise” in the radiosonde data.

Necessary conditions for the existence of clouds are:

$$T''(z) \geq 0 \quad \text{and} \quad R''(z) \leq 0, \quad z_i \leq z \leq z_j \quad (1)$$

with the requirement that the sign of the corresponding second derivative be changed at the boundary altitudes and z_j . The magnitude of the second derivatives in Equation (1) is not important. $R''(z) < 0$ means that a local maximum of relative humidity is found within a cloudy layer, as should be expected. $T''(z) > 0$ means that a local minimum of temperature is found below the cloud top. Therefore z_i and z_j are the *inflection points* of the $T(z)$ and $R(z)$ profiles and the *local extremum points* of the $T'(z)$ and $R'(z)$ profiles (i.e. maximum $R'(z)$ and minimum $T'(z)$ are to be found at z_i and minimum $R'(z)$ and maximum $T'(z)$ can be found at z_j).

In each layer satisfying the conditions described by Equation (1), the minimum dewpoint depression ($T - T_d$), i.e. the difference between the air temperature (T) within the cloudy layer and the corresponding dew point (T_d), is determined using the expressions given below⁵:

$$T_d = \frac{5420}{\ln\left(\frac{2.53 \times 10^{11}}{R e_s}\right)} - 273.15 \quad (\text{°C}) \quad (2)$$

where

R is the relative humidity reported as a fractional number;

e_s is the saturation vapour pressure of pure water vapour over a plane surface of liquid water, evaluated using the AERK approximation found in Alduchov and Eskridge⁶:

$$e_s = 610.94 e^{(17.625T)/(243.04+T)} \quad (\text{Pa}) \quad (3)$$

where T is the air temperature in degrees Celsius.

The CE method uses the graphical method of predicting cloud amount developed empirically by Arabey². The (T , $T - T_d$) plane is divided into four regions (see Fig. 1):

Region 1: a saturated region with cloud cover of 80%-100%;

Region 2: a nearly saturated region with cloud cover of 60%-80%;

Region 3: a drier region with cloud cover of 20%-60%;

Region 4: a region of dry air with cloud cover of 0%-20%. This region is often interpreted as a region with clear sky for thin layers.

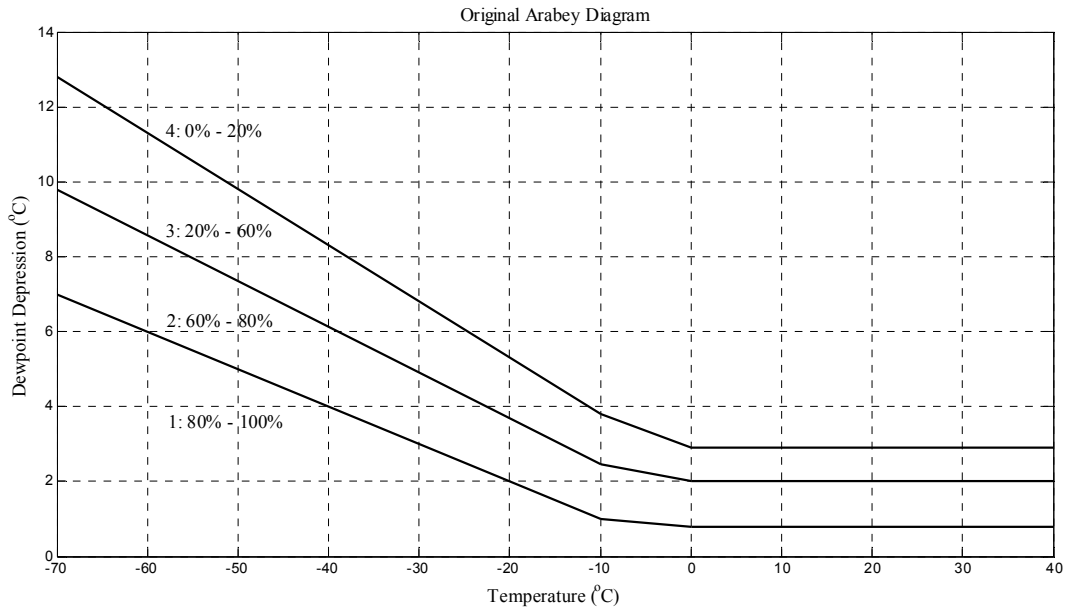


Figure 1. Piecewise linear approximation of the Arabey diagram extended to +40°C by Chernykh and Eskridge¹. The $(T, (T-T_d))$ plane is divided into four regions. *Region 1*: a saturated region with cloud cover of 80%-100%; *Region 2*: a nearly saturated region with cloud cover of 60%-80%; *Region 3*: a drier region with cloud cover of 20%-60%; *Region 4*: a region of dry air with cloud cover of 0%-20%. The latter is often interpreted as a cloudless region (i.e. clear sky).

Arabey developed this diagram for the temperature range of -70°C to $+30^{\circ}\text{C}$ by extrapolating to both lower and higher temperatures the empirical graph of Moshnikov² defined for T lying between -40°C to $+2^{\circ}\text{C}$. Arabey evaluated his method using radiosonde data from the former Soviet Union and a voyage of the vessel Akademik Korolev in the Tropical zone of the Indian Ocean. Finally Chernykh and Eskridge¹ extended the Arabey diagram to $+40^{\circ}\text{C}$ by a linear extrapolation of the linear segments used between 0°C and $+30^{\circ}\text{C}$. Table 1 presents the coefficients of the piecewise linear approximation of the Arabey diagram of the form $D = a*T + b$, where D is the dewpoint depression. The steeper lines used for $-70^{\circ}\text{C} < T \leq -10^{\circ}\text{C}$ in Table 1 can be explained by the larger time lag of the radiosondes' hygrometers in very cold air.

Table 1 Coefficients a and b for the piecewise linear approximation of the Arabey diagram using the form $D = a*T + b$, where D is the dewpoint depression. See Fig. 1.

$-70^{\circ}\text{C} < T \leq -10^{\circ}\text{C}$		$-10^{\circ}\text{C} < T \leq 0^{\circ}\text{C}$		$0^{\circ}\text{C} < T < 40^{\circ}\text{C}$	
a	b	a	b	a	b
-0.1	0	-0.02	0.8	0	0.8
-0.1225	1.225	-0.045	2.0	0	2.0
-0.15	2.3	-0.09	2.9	0	2.9

2.3 Modified CE method using supplementary data not measured by radiosondes

Relations (1) refer to necessary conditions for the presence of cloudy layers. In fact, the CE method can sometimes predict cloudy layers under clear sky (cloudless) conditions, i.e. false positives¹. For example, large peaks of relative humidity in excess of 80% sometimes occur either in the boundary layer or higher up under clear sky conditions, as will be seen in the following case.

Clear sky conditions prevailed over the CRC in Ottawa on January 18, 2005 between 14:00 and 20:15 UTC. Weather observers at the Ottawa International Airport also reported clear sky conditions between 13:00 and 21:00 UTC. Profiles of temperature, water vapour (absolute humidity), relative humidity and cloud liquid water between the surface and 10 km at 14:00 UTC for that day are shown in the right portion of Fig. 2. The profiling radiometer was retrieving profiles once every 30 seconds.

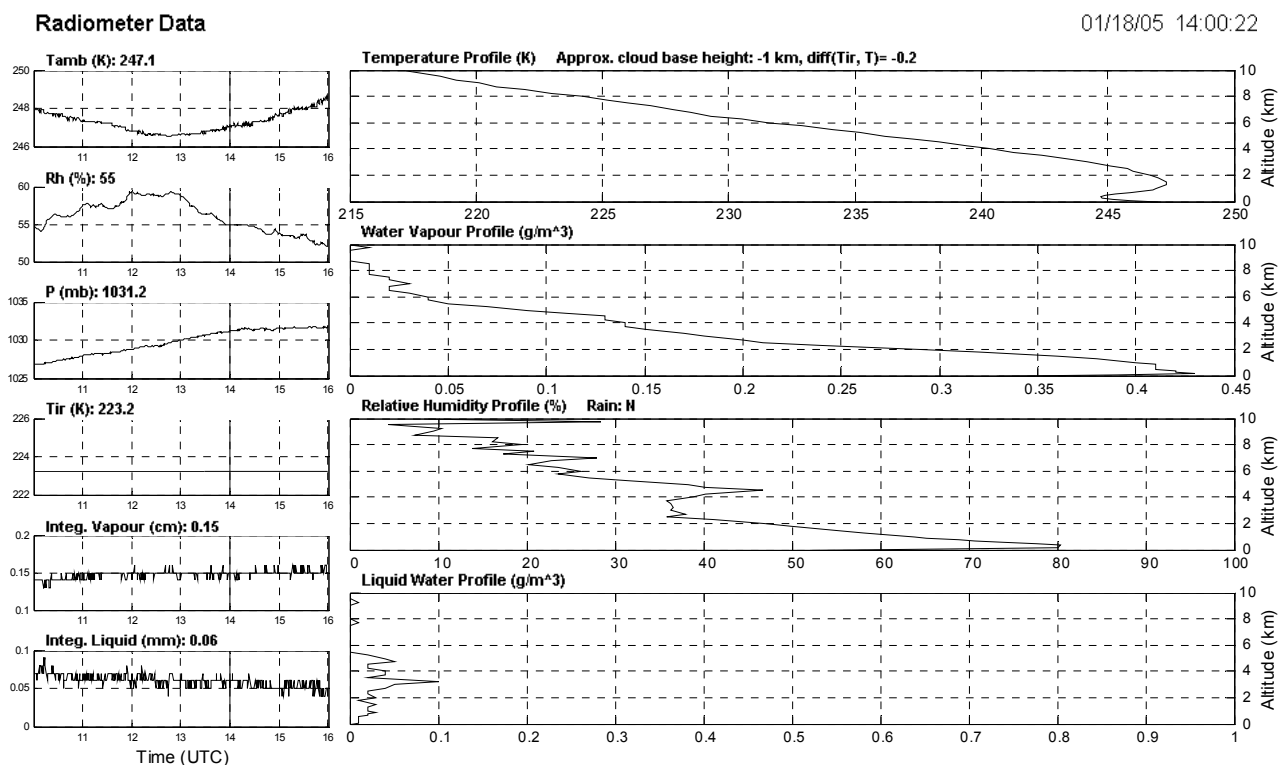


Figure 2. Retrievals on January 18, 2005 at 14:00 UTC when clear sky (cloudless) conditions prevailed over CRC. The liquid water path (“integrated liquid”) was not exactly equal to 0 mm but T_{ir} stayed at 223.2 K, providing evidence that clear sky conditions prevailed at the time. The six subplots on the left panel are time series of surface meteorological parameters and integrated retrievals. Note the large peak in the relative humidity profile (80%) between 200 m and 400 m above ground level.

Time history of surface temperature (T_{amb}), relative humidity (Rh) on the ground, pressure (P) at the surface, temperature of the cloud base (T_{ir}), water vapour path (integrated vapour) and liquid water path (integrated liquid) are shown on the left panel. Predictions based on the original CE method for January 18, 2005 between 14:00 and 14:15 UTC include a number of cloudy layers (false positives) satisfying conditions (1) between 100 m above ground (or from the surface for last few profiles) and about 1.15 km due to the large peak around 80% in the relative humidity profile between 200 m and 400 m above ground, as shown in Fig. 3.

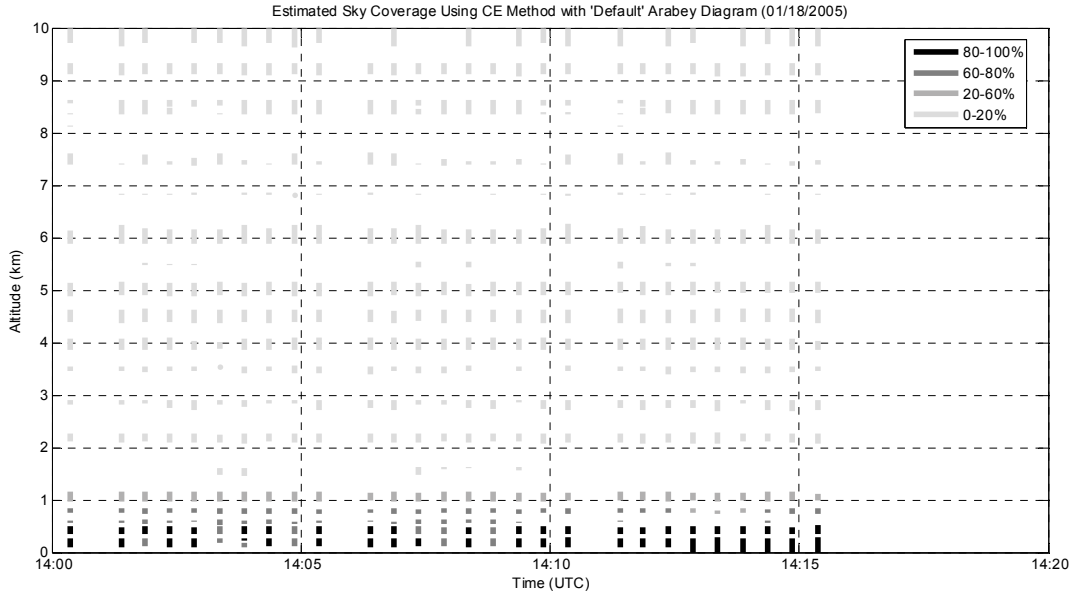


Figure 3. Predicted cloud layers using the original CE method for January 18, 2005 between 14:00 and 14:15 UTC (completely clear sky conditions). Each vertical profile shows four or five cloudy layers (false positives) satisfying conditions (1) with predicted cloud amounts ranging from 20 to 100% between 100 m above ground (or from the surface for last few profiles) and 1.15 km (in black and darker gray). All predicted layers above 1.15 km are correctly identified as being cloudless (light gray), having an estimated cloud amount lying between 0% and 20%.

Two of the various parameters measured by the profiling radiometer can be used to reduce the number of false positives predicted by the CE method: the cloud base height (CBH) of the lowest layer estimated by the zenith-looking infrared thermometer (IRT) and the liquid water path L . As mentioned earlier, the IRT operates between 9.6 and 11.5 μm and measures temperature T_{ir} . The CBH is readily estimated using T_{ir} and the contemporaneously retrieved temperature profile. The minimum detectable temperature $T_{ir\ min}$ is -50°C ; this usually corresponds to cloudless conditions. However, T_{ir} can be larger than -50°C in clear sky conditions during the summer whenever the air has water vapour paths in excess of a few centimeters. Under such conditions the retrieved CBH can be, for example, around 8 or 8.5 km.

This author presents an extra set of conditions for the existence of liquid water or mixed-phase clouds to supplement Eq. (1) in an effort to reduce the number of false positives:

$$-1 < CBH < CBH_{th} \quad \text{and} \quad L \geq L_{th} \quad (4)$$

where CBH_{th} is a maximum cloud base height for liquid water and/or mixed-phase clouds. For the case of our profiling radiometer CBH_{th} has been empirically found to be around 6 km for the cloud climatology of the Ottawa area, which corresponds approximately to the largest observed cloud base height of midlevel clouds like Altostratus. The current software of our profiling radiometer considers that there are no cloud whenever $T_{ir} < 240\text{ K}$, a condition that is noted as $CBH = -1$ in this paper.

A threshold liquid water path L_{th} is determined for each time period of interest using the cloud detection algorithm described by the flowchart in Fig. 4. It has been found that this parameter is estimated with better accuracy when the whole 24-hour data file of retrievals produced by our profiler is used, instead of a quicker search for L_{th} through the time interval of interest for the analysis of cloud cover.

It would be useful at this point to explain the genesis of this algorithm (Fig. 4). Theoretically, the second condition in Eq. (4) would be $L > 0$. This threshold liquid water path has to be determined every time the improved CE method is used since L is not always exactly equal to 0 mm under clear sky conditions due to noise in the neural network retrieval

for this parameter. The noise level varies with weather conditions at the site and the radiosonde dataset used to train the neural network. Moreover noise levels from the neural network under clear sky conditions and actual amounts of columnar cloud liquid (L) can sometimes overlap in the case of midlevel, mixed-phase or supercooled clouds, for example⁷. Turning back to Fig. 2 again, the time series of L displayed in the lower left corner of this figure provides an example of neural network noise under cold, clear sky conditions. The fact that T_{ir} was equal to 223.2 K during the time period displayed in this time series (from 10:00 to 16:00 UTC) provided evidence that clear sky conditions then prevailed.

Finally, a third parameter, the retrieved water vapour path V , is also used in this cloud detection algorithm to check for rain contamination in the data. Spurious peaks in the time series of V are a sign of rain contamination. The threshold water vapour path V_{th} in Fig. 4 is found to be around 2 cm in the winter and around 6 cm in the summer for the climate of the Ottawa area.

Application of the algorithm described in Fig. 4 together with the new Arabey diagram presented in the next section have completely eliminated false positives under completely clear sky or almost clear sky conditions (i.e. with cloud amount smaller than 25% or 2 oktas), as will be described later in this paper (see Section 5).

2.4 New Arabey diagram for the liquid water and mixed-phase cloud climatology of the Ottawa area

An Arabey diagram for the liquid water and mixed-phase clouds of the Ottawa area is shown in Figure 5. The various slopes and intercepts are presented in Table 2. This new Arabey diagram has been constructed, step by step, using the following strategy:

1. All of the 37 completely clear sky cases observed at CRC between the Fall of 2004 and the Summer of 2005 have been analyzed using the original Arabey diagram shown in Fig. 1 and described in more detail in Table 1. The slopes and the intercepts have been modified for air temperatures lower than 0°C to maximize the number of clear sky cases lying completely inside region 4 (0%-20%). In other words, region 4 of the original diagram has been enlarged for $T < 0^\circ\text{C}$. Difficult clear sky cases (11 out of the 37) with large peaks of relative humidity similar to the one illustrated in Fig. 2 (and including this very case) have been handled by the cloud detection algorithm described in Fig. 4. Most completely clear sky cases (i.e. 26 out of 37) had large dewpoint depressions and thus were handled without difficulty by the modified Arabey diagram;
2. Cases with almost clear sky with total cloud amounts of various types no larger than 25% were analyzed with this modified Arabey diagram;
3. Cases with cloud amounts between 25% and 50% were then analyzed, followed by cases of layer clouds like Stratocumulus and Stratus covering 75% to 100% of the sky;
4. Cases where two liquid water cloud layers (for example, Altocumulus clouds overlying Stratocumulus) have been observed over CRC were analyzed.

The zones of the new Arabey diagram have been slightly modified so as to be consistent with the established practice of dividing the celestial dome into 8 portions (oktas) used by weather observers in Canada. Therefore 0%-20% became 0%-25% (0/8-2/8); 20%-60% became 25%-63% (2/8-5/8), etc.

With the exception of the 0%-25% zone (clear sky or almost clear sky zone), the new diagram is valid down to -40°C since liquid water clouds cannot exist at temperatures lower than the temperature of homogeneous nucleation⁵. Moreover the profiling radiometer is not sensitive to Cirrus clouds assumed to be entirely composed of ice crystals.

The slopes and intercepts for air temperatures larger than 0°C found in the two rightmost columns of Table 1 have been left untouched in the new Arabey diagram (see Table 2) since they agreed well with the observed cloud cover data.

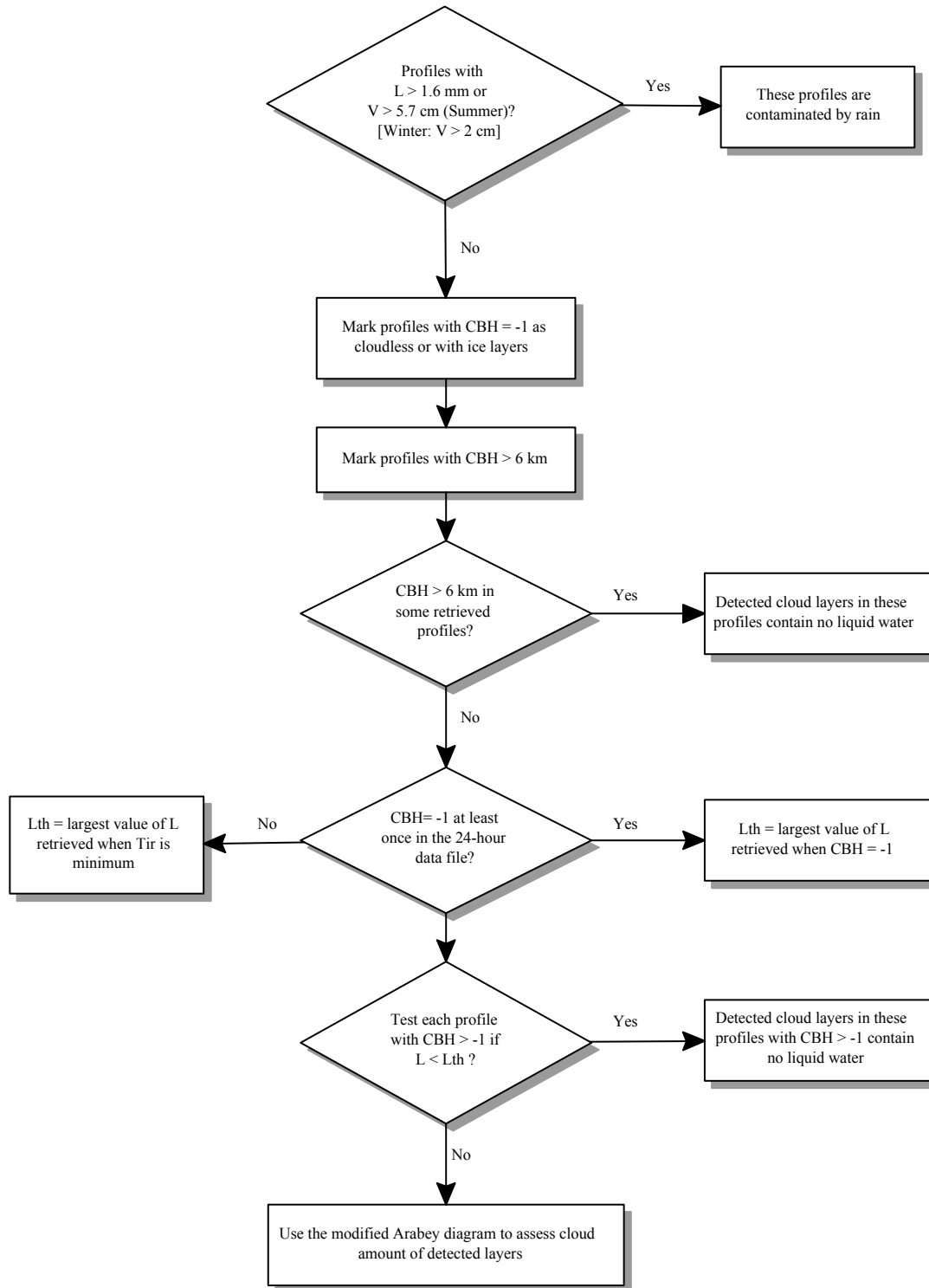


Figure 4. Flowchart for the proposed liquid cloud detection algorithm to reduce the number of false positives. L is the retrieved liquid water path, V is the water vapour path and T_{ir} is the temperature measured by the infrared radiometer. CBH is the cloud base height. Note that $CBH = -1$ whenever $T_{ir} < 240$ K.

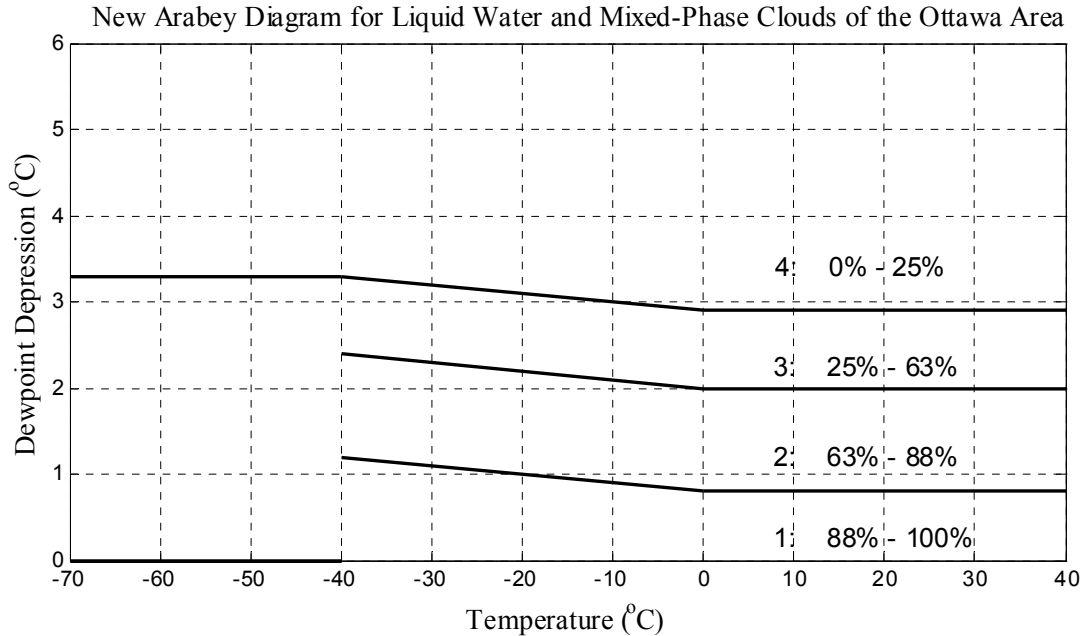


Figure 5. New Arabey diagram for the liquid water and mixed-phase cloud climatology of the Ottawa area. The $(T, (T-T_d))$ plane is still divided into four regions. *Region 1*: a saturated region with cloud cover of 88%-100%; *Region 2*: a nearly saturated region with cloud cover of 63%-88%; *Region 3*: a drier region with cloud cover of 25%-63%; *Region 4*: a region of dry air with cloud cover of 0%-25%. This region is usually interpreted as a cloudless region (i.e., clear sky). With the exception of Region 4, all regions are defined for air temperatures between -40°C and 40°C , since liquid water clouds cannot exist at temperatures lower than -40°C .

Table 2. Coefficients a and b for the piecewise linear approximation of the new Arabey diagram for the liquid water and mixed-phase cloud climatology of the Ottawa area using the form $D = a*T + b$, where D is the dewpoint depression. See Fig. 5.

$-70^{\circ}\text{C} < T \leq -40^{\circ}\text{C}$		$-40^{\circ}\text{C} < T \leq 0^{\circ}\text{C}$		$0^{\circ}\text{C} < T < 40^{\circ}\text{C}$	
a	b	a	b	a	b
0	0	-0.01	0.8	0	0.8
0	0	-0.01	2.0	0	2.0
0	3.3	-0.01	2.9	0	2.9

3. DATA

The data set used consists of the author's daytime observations of cloudiness over the profiling radiometer deployed at the CRC in Ottawa. It covers the period between the fall of 2004 and the summer of 2005. Earlier data from 2003 have been omitted here since both hardware and software upgrades to the profiler done at the factory during the summer of 2004 have resulted in much improved humidity profiles (i.e. reaching saturation within the cloud layer(s)) for low-lying clouds like Stratocumulus. Due to time constraints, cloud cover observations during precipitation – either rain, drizzle or even light snow – have been omitted from the analysis presented here.

4. CASE STUDY

A brief case study will be presented here to show the capabilities of the CE method. Another case study will be presented at the Symposium.

On June 29, 2005, this author observed a layer of Stratocumulus (Sc) covering the whole sky over CRC in Ottawa between 19:26 and 19:31 UTC. A sharp Sun was visible through the layer, providing evidence that this was indeed the correct cloud type⁸. Moreover, surface weather observers at the Ottawa International Airport reported a layer of Sc associated with Cumulus covering 7/8 of the sky with a base at 1.3 km at 19:00 UTC. They reported the same cloud at 20:00 UTC, but this time with opacity of 6/8 and a base at 1.6 km.

Figure 6 presents a time series of cloud layers predicted by the CE method for that case. The profiling radiometer was retrieving vertical profiles every minute at the time. Circles indicate the cloud base height estimated by the profiler's infrared thermometer (T_{ir}). These were consistent with the above-mentioned observations at the Airport at 19:00 and 20:00 UTC. Following Chernykh and Eskridge¹, moist layers with cloud amounts larger than 25% lying below the cloud base height estimated by infrared thermometer (shown as circles in Fig. 6) were ignored in the analysis. Each vertical profile typically showed a cloud with a thickness of about 850 m and a cloud amount falling either in the (88%-100%) zone in black at 19:26, 19:29 and 19:30 UTC, or in the (63%-88%) zone in dark gray for the other three profiles. Light gray layers were considered cloudless, having an estimated cloud amount lying between 0% and 25%. All six cloudy profiles passed the test of the liquid cloud detection algorithm described in Fig. 4.

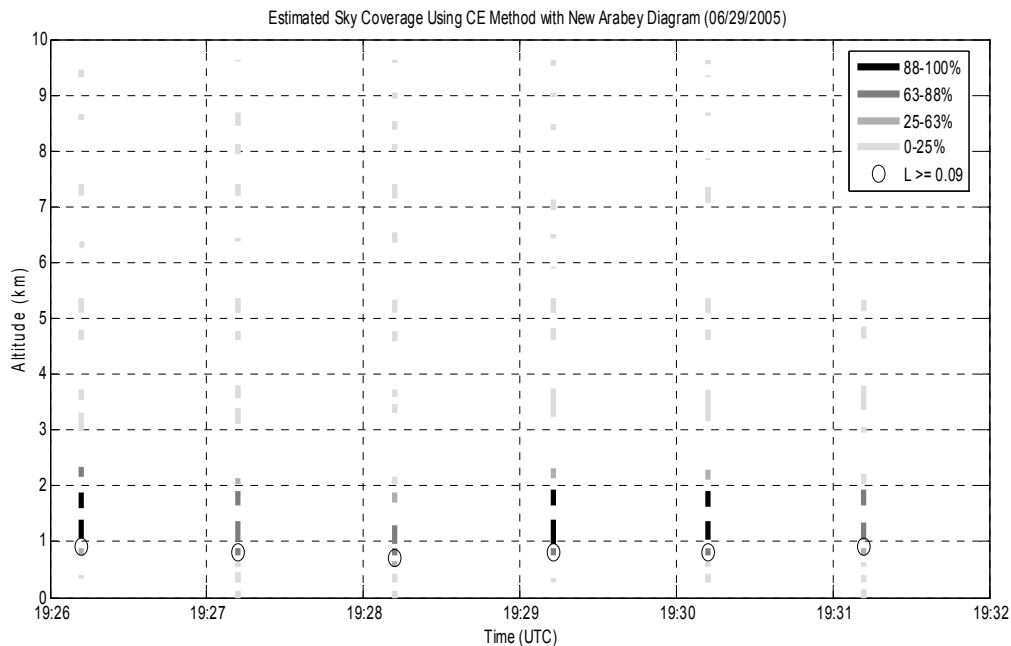


Figure 6. Predicted cloud layers using the modified CE method for June 29, 2005 between 19:26 and 19:31 UTC. A layer of Stratocumulus covered the whole sky (8/8) over the CRC. Circles indicate cloud base height estimated by the profiling radiometer's infrared thermometer. The retrieved liquid water path ranged from 0.14 to 0.19 mm. Each vertical profile typically shows a cloud with a total thickness of about 850 m and a cloud amount falling either in the (88%-100%) zone in black or in the (63%-88%) zone in dark gray. Light gray layers are considered cloudless, having an estimated cloud amount lying between 0% and 25%.

5. RESULTS

Results have been compiled using a simple “hit” or “miss” criterion: a hit meant that both cloud layers and amounts were consistent with recorded sky observations at CRC and METARs from the Ottawa International Airport. Retrieved cloud base heights were also used to check consistency. A “miss” meant that the improved CE method failed to detect the correct cloud amounts at the appropriate altitude(s). Cases with Cumulus clouds were considered successful (i.e. a “hit”) when there was at least one profile within the observation period with the right cloud amount and base height since the profiling radiometer can typically sense these modest-size clouds only for a few minutes.

Table 3 presents success rates with both the original and the modified CE method.

Table 3. Success rates with both the original and the modified CE method for non-precipitating clouds over CRC (Ottawa). Standard WMO cloud genera are used in this paper. Ac: Altocumulus; As: Altostratus; Ci: Cirrus; Cu: Cumulus; Sc: Stratocumulus; St: Stratus.

Cloud Type (non-precipitating)	Time period	Number of Cases	Success Rate with the Original CE method	Success Rate with the Modified CE method (New Arabey diagram + Liquid Cloud Detection Algorithm)
None (Clear Sky)	Dec. 2004-Aug. 2005	37	46 %	100 %
Mostly clear sky with total cloud amount of either Ac, Cu, Sc, St or Ci \leq 25%	Oct. 2004-Aug. 2005	95	49 %	100 %
Cu with cloud amount $>$ 25%	May 2005-Aug. 2005	15	60 %	60 %
Sc with cloud amount \geq 75%	April 2005-Aug. 2005	17	94 %	94 %
Ac with cloud amount \geq 88%	Feb. 2005-Aug. 2005	10 but two glaciated	75 %	88 %
Overcast As	Nov. 2004, Dec. 2004 and Feb. 2005	11 but one glaciated case	70 %	70 % <i>(usually more accurate predictions than the original CE method)</i>
Ac over Sc (Two layers)	May 2005-Aug. 2005	13	85 %	85 %

The success rate obtained with the original CE method for clear sky conditions (46%) is fairly consistent with results presented in Table 1, column P1, of their original paper (Reference 1). The liquid cloud detection algorithm shown in Fig. 4 eliminated false positives in all of 132 cases of clear sky and mostly clear sky conditions that we have analyzed. As expected, this algorithm was fairly transparent for the other cases shown in Table 3, with the exception of Altocumulus cases with cloud amounts larger or equal to 88% (nearly overcast conditions). Some cases from the late fall 2004 and winter 2005 have been included in Table 3 for midlevel clouds (Altocumulus and Altostratus). Glaciated clouds were excluded from the computation of the success rates since the profiling radiometer cannot detect these. Success rates were high for both the low-lying Stratocumulus and the two-layer cases.

6. CONCLUSIONS

Below are the main conclusions reached during the course of this research on cloud detection using a ground-based multifrequency profiling radiometer:

- The CE method can be successfully applied to low and midlevel cloud cases as well as clear sky conditions using the smoother retrieved profiles of temperature and relative humidity;
- We can estimate the thickness of various layers of liquid or mixed-phase clouds present using this method. The cloud vertical structure is a key parameter for modeling the radiowave attenuation due to cloud liquid water;
- High (cirriform) ice clouds and glaciated midlevel winter clouds can be detected by the profiler's infrared thermometer if their cloud base temperatures are greater than 223.2 K but cannot be analyzed with the CE method using retrievals from our profiling radiometer. This can be explained by the fact that the imaginary part of the complex refractive index of ice is very much smaller than that of liquid water at microwave frequencies;
- A new cloud detection algorithm based on the use of supplementary data not measured by radiosondes (the retrieved liquid water path (L) and the cloud base height measured by the profiler's infrared thermometer) has been shown to significantly reduce the number of false positives;
- A new Arabey diagram for the water cloud climatology of the Ottawa area has also been presented. It appears that the diagram had to be modified for air temperatures lower than 0°C in order to be applicable to profiles of temperature and relative humidity retrieved by our multifrequency radiometer.

REFERENCES

1. I. V. Chernykh and R. E. Eskridge, "Determination of cloud amount and level from radiosonde soundings," *Journal of Applied Meteorology*, **35**, pp. 1362–1369, 1996.
2. E. N. Arabey, "Radiosonde sounding data as a tool for investigating cloud layers," *Meteorol. Gidrol.*, **6**, pp. 32-37, 1975 (in Russian).
3. I. V. Chernykh and O. A. Alduchov, "Vertical distribution of cloud layers from atmospheric radiosounding data," *Izvestiya, Atmospheric and Oceanic Physics*, **40**, pp. 41-53, 2004.
4. R. L. Burden and J. D. Faires, *Numerical Analysis*, PWS-Kent, Boston, 1989.
5. R. R. Rogers and M. K. Yau, *A Short Course in Cloud Physics*, Pergamon Press, New York, 1989.
6. O. A. Alduchov and R. E. Eskridge, "Improved Magnus form approximation of saturation vapor pressure," *Journal of Applied Meteorology*, **35**, pp. 601–609, April 1996.
7. Z. Wang, K. Sassen, D. N. Whiteman, and B. B. Demoz, "Studying Altocumulus with ice virga using ground-based active and passive remote sensors," *Journal of Applied Meteorology* **43**, pp. 449–460, 2004.
8. J. R. Linskens and C. F. Bohren, "Appearance of the Sun and the Moon seen through clouds," *Appl. Opt.*, **33**, pp. 4733-4740, 20 July 1994.